

Pre-equilibrium Neutron Emission in Fission or Fragmentation

Aurel Bulgac^{1,*}

¹*Department of Physics, University of Washington, Seattle, Washington 98195-1560, USA*

(Dated: September 11, 2020)

Fissioning nuclei and fission fragments, nuclear fragments emerging from energetic collisions, or nuclei probed with various external fields can emit one or more pre-equilibrium neutrons, protons, and potentially other heavier nuclear fragments. I describe a formalism which can be used to evaluate the pre-equilibrium neutron emission probabilities and the excitation energies of the remnant fragments.

I. INTRODUCTION

Instances when particles are emitted or knocked-out of a quantum system after probing those systems are ubiquitous. In the Auger-Meitner effect [1, 2] in atoms, when an inner shell electron is removed, the left behind hole state is filled by an electron from a higher energy level and the energy released is used to eject another electron. In nuclear physics the ejection of a deeply bound proton in a $(e, e'p)$, $(p, 2p)$ or in a relativistic Coulomb excitation reaction is often accompanied by the emission of an additional nucleon. When a nucleus undergoes either a β - or α -decay, the change of the Coulomb field of the nucleus leads to electron ionization [3]. In fission, at scission immediately after the neck rupture the fission fragments are in each other's repulsive Coulomb fields and start accelerating and the single-particle potential experienced by nucleons changes [4–10], see also Fig. 1. The reference framework of each fission fragment is a non-inertial one and the equilibrium of the nuclear fluid is disturbed in a similar manner to what happens to water in an accelerated container. The nuclear matter accumulates at first near the edges of the fission fragments facing each other and at the same time the protons in the fragments are pushed towards the opposite edges. As a result both isoscalar and isovector vibrational modes are excited in both fragments [11, 12]. Nucleons are partially promoted onto unoccupied orbitals and a fraction of them onto unbound orbitals. The nucleons in the unbound orbitals can evaporate, in a similar fashion to the evaporative cooling method used for decades in cold atom experiments [13–21]. The goal here is to estimate the number and the probability of emitting one or more pre-equilibrium neutrons while the fission fragments are Coulomb accelerated. The formalism described here, while has number of similarities with previous studies quoted above, it clarifies the role of various approximations used and it is also extended in a number of ways the range of previously not considered in literature observables.

II. PROBABILITIES OF PRE-EQUILIBRIUM NEUTRON EMISSION

The time evolution of the neutrons is described by a time-dependent Slater determinant $\Phi(x_1, \dots, x_N, t)$ within a energy density functional approach, which is built from the time-dependent single-particle wave functions $\phi_k(x, t)$ with $k = 1, \dots, N$, which are solutions of the evolution time-dependent equations

$$i\hbar \frac{\partial \phi_k}{\partial t} = h\phi_k, \quad (1)$$

where h is the time-dependent mean field single-particle Hamiltonian. One can consider pre-equilibrium neutrons emitted for example from a Coulomb excited nucleus or from a fragment in a nucleus breakup, before a compound nucleus is formed. One possible approximation is to treat the excitation within the Random Phase Approximation (RPA), which is the small amplitude limit of the Hartree-Fock approximation or of the Density Functional Theory (DFT). If the nucleus is weakly excited then the RPA is valid and it should be in good agreement with the full DFT approach, which is considered here.

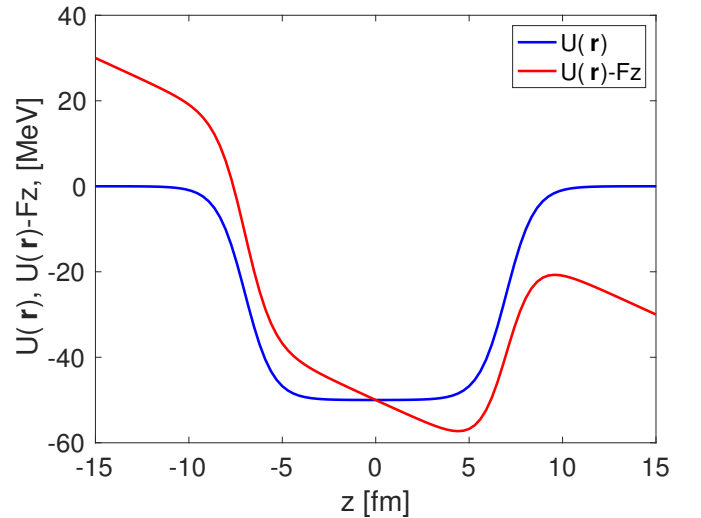


FIG. 1. (Color online) The profile of the potential experienced by nucleons at rest (black line) and of an uniformly accelerated one (red line) with acceleration $a = F/m$ in the z -direction.

* bulgac@uw.edu

I will concentrate at first on the case of a single nuclear fragment and discuss the case of two fragments below, see Eqs. (35) and (37). The neutrons populate $M > N$ bound single-particle orbitals $\psi_n(x)$ in a fragment and $M+1, \dots, \infty$ unbound orbitals in a final fragment moving with the velocity \mathbf{v}

$$\mathbf{v}_{L,R}(t) = \frac{1}{Nm} \langle \Phi | \hat{P}_{L,R} \sum_{k=1}^N \hat{\mathbf{p}}_k \hat{P}_{L,R} | \Phi \rangle, \quad (2)$$

where $\hat{\mathbf{p}}_k = -i\hbar\nabla_k$ is the momentum operator, m the nucleon mass, and

$$\hat{P}_{L,R}(N) = \int_{-\pi}^{\pi} \frac{d\eta}{2\pi} e^{i\eta(\hat{N}_{L,R}-N)}, \quad (3)$$

$$N_{L,R} = \int d\xi \Theta(\mp z) \sum_{n=1}^A |\phi_n(\xi)|^2, \quad (4)$$

where $\xi = \mathbf{r}, \sigma$ stands for spatial $\mathbf{r} = (x, y, z)$, spin $\sigma = \uparrow, \downarrow$, and isospin $\tau = n, p$ coordinates, and the sum is over occupied single-particle states, is a projector onto a specific final nuclear fragment (the one of the left or the one on the right). Note that this projector $\hat{P}_{L,R}$ [22–24] simply defines the part of the space where one fission fragment ends up (basically $\Theta(\pm z)$ identifies the part of the volume where one or the other fragment is after scission, and it is different from the projector $\hat{\mathcal{P}}$ introduced below.

I introduce now two projectors onto the final single-particle states of a fragment, resulting after pre-equilibrium neutrons have been emitted. These projectors can be thought of as de facto analyzers of the fission fragment structure. For example, at scission a typically highly excited fragment with N_f neutrons was formed. This fission fragment can emit a number of pre-equilibrium neutrons n , after which the remaining fragment will eventually turn into a compound nucleus with $n' = N_f - n$ neutrons, from which neutrons and gammas can be emitted statistically. In the first approximation one can assume that n is small enough and $n' \approx N_f$, an approximation which can be improved iteratively. I will assume for now that no protons have been emitted after scission, an assumption which can be easily released if necessary. These projectors are designed to analyze the character of the single-particle content of a fission fragment, specifically whether the single-particle orbitals are bound ($k = 1, \dots, M$) or unbound or unbound ($k > M$):

$$\hat{\mathcal{P}} = \sum_{k>M} |\psi_k^{\mathbf{v}}\rangle \langle \psi_k^{\mathbf{v}}|, \quad \hat{\mathcal{Q}} = \sum_{k=1}^M |\psi_k^{\mathbf{v}}\rangle \langle \psi_k^{\mathbf{v}}|, \quad (5)$$

where $\psi_k^{\mathbf{v}}(x) = \exp(i\mathbf{m}\mathbf{v}\cdot\mathbf{r}/\hbar)\psi_k(x)$ with $x = \mathbf{r}, \sigma$ are defined in the reference frame moving with velocity $\mathbf{v}(\mathbf{r}, t)$ ¹

¹ In the case of ²⁴⁰Pu induced fission the fragments carry on av-

and

$$\hat{\mathcal{P}} + \hat{\mathcal{Q}} = \mathbb{1}. \quad (6)$$

The single-particle wave functions $\psi_k(x)$ describe a final stationary nucleus or fission fragment in its ground state onto which one wants to project the time evolved single-particle wave functions $\phi_k(x, t)$.

Following a line of argument similar to the formalism described in Refs. [22, 23] one can show that the probability to have n unbound neutrons is given by

$$P(n) = \int_{-\pi}^{\pi} \frac{d\eta}{2\pi} \langle \Phi | \exp[i\eta(\hat{\mathcal{P}} - n)] | \Phi \rangle \quad (7)$$

$$= \int_{-\pi}^{\pi} \frac{d\eta}{2\pi} e^{-i\eta n} \det[\delta_{kl} + (e^{i\eta} - 1)\langle \phi_k | \hat{\mathcal{P}} | \phi_l \rangle], \quad (8)$$

and the probability that the rest of the $n' = N - n$ neutrons will be in the M bound states is

$$Q(n') = \int_{-\pi}^{\pi} \frac{d\eta}{2\pi} e^{-i\eta n'} \det[\delta_{kl} + (e^{i\eta} - 1)\langle \phi_k | \hat{\mathcal{Q}} | \phi_l \rangle], \quad (9)$$

and where

$$\langle \phi_n | \hat{\mathcal{P}} | \phi_m \rangle + \langle \phi_n | \hat{\mathcal{Q}} | \phi_m \rangle = \delta_{nm}. \quad (10)$$

These formulas assume that the fission fragments were followed in time sufficiently far enough that their accelerations at times greater than t would lead to only negligible further excitations of the nucleons into unbound orbitals and hopefully also the one-body mechanism ceased to be effective [25–27]. Since a Slater determinant is invariant under a unitary transformation among single-particle orbitals one can always diagonalize simultaneously the two overlap matrices $\langle \phi_n | \hat{\mathcal{P}} | \phi_m \rangle$ and $\langle \phi_n | \hat{\mathcal{Q}} | \phi_m \rangle$ and obtain for the probabilities $P(n)$ and $Q(n)$ simpler formulas

$$\langle \phi_k | \hat{\mathcal{P}} | \phi_l \rangle = \alpha_k^2 \delta_{kl}, \quad \langle \phi_k | \hat{\mathcal{Q}} | \phi_l \rangle = \beta_k^2 \delta_{kl}, \quad (11)$$

$$\alpha_k^2 + \beta_k^2 = 1, \quad (12)$$

$$P(n) = \int_{-\pi}^{\pi} \frac{d\eta}{2\pi} e^{-i\eta n} \prod_{k=1}^N [1 + (e^{i\eta} - 1)\alpha_k^2], \quad (13)$$

$$Q(n') = \int_{-\pi}^{\pi} \frac{d\eta}{2\pi} e^{-i\eta n'} \prod_{k=1}^N [1 + (e^{i\eta} - 1)\beta_k^2]. \quad (14)$$

In the case of fission fragments the orbitals $\psi_k(x)$ with $k \leq M$ can describe the bound states in either only one or in both fission fragments. Thus one can separate the

erage about 0.7 MeV kinetic energy per nucleon, which amounts to a wave vector $k \approx 0.2 \text{ fm}^{-1}$. In this case $e^{ikR} \approx 0.36 + i0.93$ and $e^{ikd} \approx -0.73 + i0.68$, where $d = 2R \approx 12 \text{ fm}$ is the average fission fragment diameter. Consequently the correct values of the overlaps $\langle \phi_k | e^{i\mathbf{k}\cdot\mathbf{r}} | \psi_l \rangle$ can be noticeable different from an approximate estimate $\langle \phi_k | \psi_l \rangle$.

number of neutrons emitted from each fragment. Note that in order to calculate $P(n)$ and $Q(n)$ only the overlaps $\langle \phi_k | \hat{Q} | \phi_l \rangle$ between the bound orbitals are needed.

It is useful to introduce the generating functions for the moments $\langle n^l \rangle$ and cumulants $\langle\langle n^l \rangle\rangle$ [28, 29], which for the $P(n)$ probability distribution are

$$G_P(\tau) = \prod_{k=1}^N [1 + (e^\tau - 1)\alpha_k^2] = \sum_{l=0}^{\infty} \frac{\tau^l}{l!} \langle n^l \rangle, \quad (15)$$

$$\ln G_P(\tau) = \sum_{l=0}^{\infty} \frac{\tau^l}{l!} \langle\langle n^l \rangle\rangle, \quad (16)$$

$$\langle n \rangle = \sum_{k=1}^N \alpha_k^2, \quad \langle\langle n^2 \rangle\rangle = \sum_{k=1}^N \alpha_k^2 \beta_k^2, \quad (17)$$

$$\langle\langle n^3 \rangle\rangle = \sum_{k=1}^N \alpha_k^2 \beta_k^2 (\beta_k^2 - \alpha_k^2), \quad (18)$$

$$\langle\langle n^2 \rangle\rangle \leq \langle n \rangle, \quad -\langle\langle n^2 \rangle\rangle \leq \langle\langle n^3 \rangle\rangle \leq \langle\langle n^2 \rangle\rangle \quad (19)$$

and one can easily obtain symbolic expressions for higher order cumulants and similar expressions for the cumulants of the $Q(n')$ probability distribution. Two potential distributions of α_k^2 are displayed in Fig. 2. As expected [22] the probabilities $P(n)$ and $Q(n')$ are correctly normalized and one can introduce the average pre-equilibrium neutron number and its variance

$$\sum_{n=0}^{\infty} P(n) = \sum_{n'=0}^{\infty} Q(n') = 1, \quad (20)$$

$$\nu = \langle n \rangle = \sum_{n=0}^{\infty} n P(n), \quad (21)$$

$$\langle\langle n^2 \rangle\rangle = \sum_{n=0}^{\infty} (n - \langle n \rangle)^2 P(n). \quad (22)$$

Additionally, equivalent formulas for $P(n)$ can be derived

$$P(0) = \prod_{k=1}^M \beta_k^2, \quad (23)$$

$$P(1) = P(0) \sum_{k=1}^M \frac{\alpha_k^2}{\beta_k^2}, \quad (24)$$

$$P(2) = P(0) \sum_{k>l=1}^M \frac{\alpha_k^2 \alpha_l^2}{\beta_k^2 \beta_l^2}, \quad (25)$$

$$P(3) = P(0) \sum_{k>l>m=1}^M \frac{\alpha_k^2 \alpha_l^2 \alpha_m^2}{\beta_k^2 \beta_l^2 \beta_m^2}, \quad (26)$$

with similar expressions for $P(n > 3)$.

The neutron density matrix can be represented in two ways

$$\hat{n} = \sum_{k=1}^N |\phi_k\rangle \langle \phi_k| = \sum_{k=1}^N (|\alpha_k\rangle + |\beta_k\rangle)(\langle \alpha_k| + \langle \beta_k|) \quad (27)$$

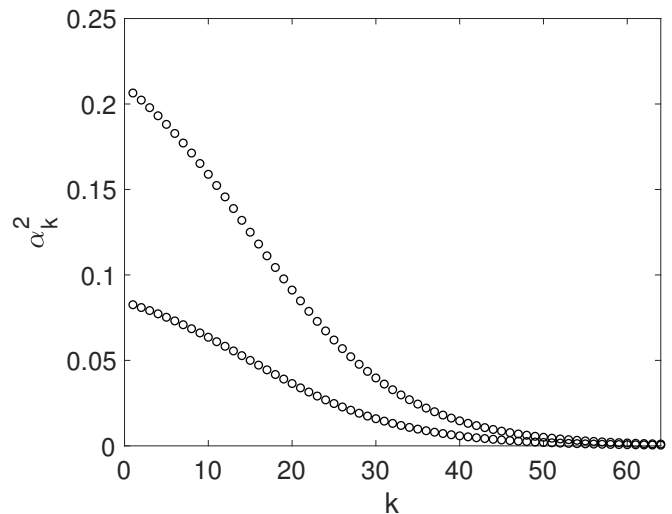


FIG. 2. (Color online) Two different α_k^2 -distributions of unoccupied overlaps α_k^2 , see Eq. (11), which differ only by their overall magnitude. α_k^2 are fractions of the single-particle occupation in orbitals $\phi_k(x, t)$ lying in the continuum. One expects that the highest lying orbitals are depleted the most and α_k^2 are then roughly ordered in reverse order of the instantaneous expectation value of the single-particle energy $\varepsilon = \langle \phi_k | h | \phi_k \rangle$, where h is the single-particle mean field Hamiltonian.

and then show that the average number of neutrons emitted by a fragment is

$$\nu = \langle \Phi | \sum_{m=1}^{\infty} P(m) | \Phi \rangle = \sum_{k=1}^N \alpha_k^2. \quad (28)$$

The knowledge of the average number of particle emitted only could incorrectly characterize the evaporation or the decay process if ν is large. One can envision a situation when $P(0) = 1 - \epsilon$ and $\sum_{n=1}^{\infty} P(n) = \epsilon \ll 1$, and $P(n)$ has a weak intensity peak at a large $n = n_{\max}$ value, which can be either narrow or wide. In such a case $\nu = \langle n \rangle$ could be for example $\mathcal{O}(1)$ or even much smaller, even though the nucleus can emit in reality sizable neutron clusters [30], but with a very low probability. This can happen if the emitted particles can form a relatively tightly bound cluster or a range of clusters, which are emitted with a very low probability, a situation typical in spontaneous fission, alpha-decay or cluster radioactivity [31, 32]. Cluster radioactivity could be described adequately by a proper choice of the wave functions $\psi_k(x)$. For example, if one were to determine the probability to form a particular type of cluster, one can choose a density profile describing two adjacent nuclei, one with the shape of the daughter and the other with shape of the emitted cluster. Using the density constrained method proposed by Cusson *et al.* [33] one can then construct a set of single-particle wave functions $\psi_k(x)$ corresponding to such a combined density profile and define the projector \hat{P} to select the clusters and determine their formation probability.

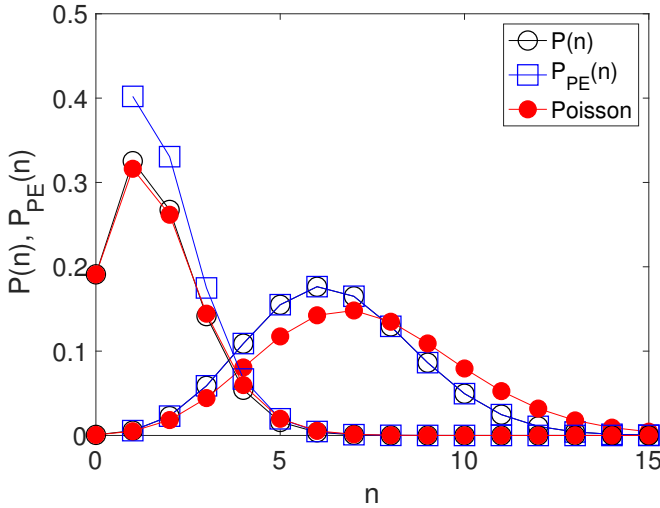


FIG. 3. This figure illustrates the corresponding probabilities $P(n)$ (13) (black circles) and $P_{PE}(n)$ (29) (blue squares) extracted using the overlap distributions from Fig. 2, and the Poisson distribution defined in Eq. (33). The α_k^2 -distribution with overall smaller magnitude leads to a peak in $P(n)$ or $P_{PE}(n)$ with $n \approx 1$, while the larger overlap α_k^2 -distribution have a maximum for $n \approx 6$. The corresponding values for ν (21) and ν_{PE} (30) for these two distributions are $\nu = 1.61$ and 6.44 , $\nu_{PE} = 1.99$ and 6.44 , and the variances $\langle n^2 \rangle$ are 1.52 and 5.06 respectively. For the Poisson distribution the mean rate $\lambda = -\ln P(0) = 1.66$ and 7.28 in these two cases and the condition $\lambda = \langle n \rangle = \langle n^2 \rangle$ is only approximately fulfilled in the case of these two α_k^2 -distributions.

Thus the evaluation of the entire probability distribution $P(n)$ and not only ν can be very informative, in order to correctly characterize the decay or evaporative process, see Fig. 3. If the probability to emit no particles $P(0)$ is not small, there will be either a weak or no correlation between ν and the value n_{\max} , where $P(n)$ is peaked and a small value of ν would merely point to a small probability to emit many nucleons, but not characterize their actual average multiplicity. I suggest to use instead the conditional probability for emitting particles and define a corrected average multiplicity neutron numbers ν_{PE} accordingly

$$P_{PE}(n) = \frac{P(n)}{\sum_{m=1}^{\infty} P(m)}, \quad (29)$$

$$\nu_{PE} = \sum_{n=1}^{\infty} n P_{PE}(n), \quad \sum_{n=1}^{\infty} P_{PE}(n) = 1. \quad (30)$$

Here $\sum_{m=1}^{\infty} P(m)$ is the probability that at least one particle is emitted. As an illustration let us consider the simple $P(n)$ distribution with $n_0 \gg 1$

$$P(n) = (1 - \epsilon)\delta_{n,0} + \epsilon\delta_{n,n_0}, \quad (31)$$

$$\nu = \epsilon n_0 \ll n_0, \quad \text{but} \quad \nu_{PE} = n_0. \quad (32)$$

A Poisson probability distribution, when the event rate is constant in time and the events are independent, can

be considered as well, and it is defined as

$$P_{\text{Poisson}}(n) = e^{-\lambda} \frac{\lambda^n}{n!}, \quad P_{\text{Poisson}}(0) = e^{-\lambda} \quad (33)$$

and it is illustrated in Fig. 3. In the case of a Poisson distribution the relations $\lambda = \langle n \rangle = \langle n^2 \rangle$ are strictly satisfied. The probability distribution $P(n)$ approaches the Poisson distribution when the average neutron multiplicity is $\nu \approx 1$ and smaller and then $\nu = \langle n \rangle \approx \langle n^2 \rangle$. The Poisson limit is satisfied strictly only in the limit $\lambda \rightarrow 0$, when

$$\lambda = \langle n \rangle = \lim_{\text{all } \alpha_k^2 \rightarrow 0} \langle n^2 \rangle = \lim_{\text{all } \alpha_k^2 \rightarrow 0} \langle n^3 \rangle. \quad (34)$$

It is not surprising that the Poisson distribution appears quite accurate in the mean field approximation and in the absence of fluctuations, see Fig. 3. One should remember however that in the present analysis the α_k^2 -distributions were considered only at a given time. Even in the mean field approximation there is no reason to expect that the evaporation rate and the α_k^2 -distributions weakly depend on time, as the one-body dissipation mechanism [25] is effective and at work even after scission [26, 27].

One can construct also the probabilities $P(n_H, n_L)$ to emit n_H and n_L neutrons from a heavy and a light fragments and study their correlations. If the projectors $\hat{Q}_{H,L}$ on the bound orbitals of either the heavy or light fragments H, L then one define the projectors $\hat{P}_{H,L} = \mathbb{1} - \hat{Q}_{H,L}$

$$P(n_H, n_L) = \int_{-\pi}^{\pi} \frac{d\eta_H}{2\pi} \int_{-\pi}^{\pi} \frac{d\eta_L}{2\pi} \langle \Phi | \exp [i\eta_H (\hat{P}_H - n_H) + i\eta_L (\hat{P}_L - n_L)] | \Phi \rangle. \quad (35)$$

While constructing these projectors one should keep in mind that the two fragments are moving with different velocities, see Eqs. (2) and (5). For well separated fragments the relations $\hat{Q}_H \hat{Q}_L = \hat{Q}_L \hat{Q}_H = 0$ and $\hat{P}_H \hat{P}_L = \hat{P}_L \hat{P}_H$ are satisfied with exponential accuracy and the final formula for $P(n_H, n_L)$ can be brought to a simple form using the relations

$$e^{i\eta_f \hat{P}_f} = e^{i\eta_f} - (e^{i\eta_f} - 1) \hat{Q}_f, \quad \text{where } f = H, L. \quad (36)$$

The average neutron multiplicity is given by

$$\nu = \nu_H + \nu_L = N - \langle \Phi | \hat{Q}_H | \Phi \rangle - \langle \Phi | \hat{Q}_L | \Phi \rangle. \quad (37)$$

These formulas for neutron emission probabilities are accurate only if the probability of emitting any protons can be neglected. This derivation assumes that the neutrons which populate the unbound states are emitted before the remnant fission fragments form a compound nuclei and are neither reabsorbed by the other fragment. A related assumption is that once a neutron is in an unbound state it is emitted before it has a chance to undergo any collisions in the fission fragment and loose

energy. The errors due to this last assumption can be accounted for by using an optical potential for the neutrons in the unbound orbitals (as in distorted wave Born approximation). A resonant single-particle state in the continuum is characterized by a total width $\Gamma = \Gamma^\uparrow + \Gamma^\downarrow$, which is related to the life-time of the state $\tau = \hbar/\Gamma$. Γ^\uparrow is the escape width and its magnitude is expected to be well described within the mean field approximation. The spreading width Γ^\downarrow characterizes the energy range over which the single-particle strength is distributed [34], due to the residual interactions and can be evaluated using an optical potential. The probability that a particle would be emitted, instead of losing its energy due to in medium collisions is proportional to the branching ratio Γ^\uparrow/Γ . Therefore one can interpret the results obtained without such corrections as upper bound estimates. An approximate way to take into account the effect of the collisions is to replace

$$\alpha_k^2 \rightarrow \alpha_k^2 \times \frac{\Gamma^\uparrow}{\Gamma^\uparrow + \Gamma^\downarrow}, \quad (38)$$

assuming that the spreading width Γ^\downarrow has a weaker energy dependence and the branching ratio is estimated at the average energy of the orbital α_k^2 .

Protons are also excited and can be in principle emitted as well, but most likely only if the corresponding occupied orbitals are above the proton Coulomb barrier. The pre-equilibrium proton emission probabilities can be estimated in the same manner. Pre-equilibrium proton emission can be neglected only if the corresponding probability to have all the protons in single-particle states with energies below the Coulomb barrier is $P(0) \approx 1$.

Another limitation of the present approach is the neglect of the role of fluctuations, see Refs. [35–38] and references therein.

After the pre-equilibrium neutrons have been evaporated and the fission fragments are fully accelerated, the excitation energy of the remnant fission fragments can be used to emit neutrons and gammas from the formed compound nucleus or fission fragments. The number of neutrons remaining in either the heavy or the light frag-

ment is

$$N_{H,L} = \sum_{k=1}^N \langle \phi_k | \hat{Q}_{H,L} | \phi_k \rangle \quad (39)$$

One can determine the occupation probabilities v_k^2 in a final fragment in its ground state in the Bardeen-Cooper-Schrieffer (BCS) approximation, under the constraint $\sum_{k=1}^M v_k^2 = N_{H,L}$, and estimate the excitation energy of such a fragment

$$E_{H,L}^* = \sum_{k=1}^M [\langle \beta_k | h | \beta_k \rangle - v_k^2 \epsilon_k]. \quad (40)$$

In deriving this approximate formula I assumed that the change in the energy is due only to the redistribution of occupation probabilities and that the densities in the ground and excited states are basically identical. This assumption is similar in spirit to the calculation of the shell energy corrections due to Strutinsky [39, 40].

All these formulas derived above implicitly assume that the average number of neutrons remaining in the fragments after evaporation $N_{L,R}$ are known in order to generate the single-particle wave functions $\psi_k(x)$. It is also implied that there exist a separation of time scales, namely one assumes that the evaporation time - which can noticeably be affected by the presence of the centrifugal barrier - is shorter than the time needed to form a compound nucleus. The wave functions $\psi_k(x)$ naturally depend on the size of the fragment, which are needed in order to evaluate $N_{L,R}$ and $nu_{L,R}$, which satisfy the sum rule

$$N = N_H + N_L + \nu_H + \nu_R. \quad (41)$$

As typically the number of evaporated neutrons $\nu_{H,L}$ is relatively small, one can neglect such details. Alternatively one can repeat the calculation once the approximate values of $N_{L,R}$ have been determined. It is likely that convergence can be achieved in one or two iterations at most. If however the number of pre-equilibrium neutrons is relatively large one might need to repeat such a procedure each time after a small number of neutrons are emitted.

Within a Hartree-Fock-Bogoliubov (HFB) framework the quasi-particle wave functions (qpwf) satisfy the equations

$$i\hbar \frac{\partial}{\partial t} \begin{pmatrix} u_{k\uparrow} \\ u_{k\downarrow} \\ v_{k\uparrow} \\ v_{k\downarrow} \end{pmatrix} = \begin{pmatrix} h_{\uparrow\uparrow} - \mu & h_{\uparrow\downarrow} & 0 & \Delta \\ h_{\downarrow\uparrow} & h_{\downarrow\downarrow} - \mu & -\Delta & 0 \\ 0 & -\Delta^* & -(h_{\uparrow\uparrow}^* - \mu) & -h_{\uparrow\downarrow}^* \\ \Delta^* & 0 & -h_{\downarrow\uparrow}^* & -(h_{\downarrow\downarrow}^* - \mu) \end{pmatrix} \begin{pmatrix} u_{k\uparrow} \\ u_{k\downarrow} \\ v_{k\uparrow} \\ v_{k\downarrow} \end{pmatrix}, \quad (42)$$

where we have suppressed the spatial \mathbf{r} and time co-

ordinate t , and k labels the qpwf $[u_{k\sigma}(\mathbf{r}, t), v_{k\sigma}(\mathbf{r}, t)]$,

with the z-projection of the nucleon spin $\sigma = \uparrow, \downarrow$. The single-particle Hamiltonian $h_{\sigma\sigma'}(\mathbf{r}, t)$, and the pairing field $\Delta(\mathbf{r}, t)$ are functionals of various neutron and proton densities, which are computed from the qpws, and μ is the chemical potential, see Ref. [41] for technical details.

Now we have to construct the projectors onto the final (stationary) nucleus determined in a mean field approximation. I assume that after scission a fragment with N_f neutrons has been formed and n pre-equilibrium neutrons are emitted and a remnant with $n' = N_f - n$ neutrons was formed. We will construct the ground state of the nucleus with n' neutrons, and assume that no pre-equilibrium protons were emitted after scission. In a first approximation one can assume that n is small enough and $n' \approx N_f$. The quasi-particle eigenstates with $E_k > 0$ (designed as occupied quasi-particle states) are typically used to construct the nucleon densities and the eigenstates with $E_k < 0$ describe the unoccupied quasi-particle states. For $E_k > 0$ the v -components and for $E_k < 0$ the u -components of the qpws have a finite norm respectively. If $\mu < E_k < -\mu$ (as $\mu < 0$ in finite nuclei) both v - and u -components have a finite norm [42–45] and the spectrum is discrete. The projectors $\hat{\mathcal{P}}$ and $\hat{\mathcal{Q}}$ to unbound and bound v -orbitals respectively are

$$\hat{\mathcal{P}} = \sum_{E_k < \mu} |\psi_k^v\rangle\langle\psi_k^v|, \quad \hat{\mathcal{Q}} = \sum_{E_k > \mu} |\psi_k^v\rangle\langle\psi_k^v|, \quad (43)$$

$$\hat{\mathcal{P}} + \hat{\mathcal{Q}} = \mathbb{1}, \quad (44)$$

where now

$$\psi_k^v(\mathbf{r}, \sigma) = \begin{pmatrix} u_{k\uparrow}(\mathbf{r})e^{\frac{im\mathbf{v}\cdot\mathbf{r}}{\hbar}} \\ u_{k\downarrow}(\mathbf{r})e^{\frac{im\mathbf{v}\cdot\mathbf{r}}{\hbar}} \\ v_{k\uparrow}(\mathbf{r})e^{-\frac{im\mathbf{v}\cdot\mathbf{r}}{\hbar}} \\ v_{k\downarrow}(\mathbf{r})e^{-\frac{im\mathbf{v}\cdot\mathbf{r}}{\hbar}} \end{pmatrix}, \quad (45)$$

as under a boost the u - and v -components of the qpws transform in opposite manner [46, 47]. This aspect is also manifest in the structure of the time-dependent density functional theory (TDDFT) Eqs. (42), as the single particle Hamiltonian changes under a boost as $h_{\sigma,\sigma} \rightarrow h_{\sigma,\sigma} + \mathbf{v} \cdot \hat{\mathbf{p}}$ [46].

The projector $\hat{\mathcal{Q}}$ projects on both occupied and unoccupied bound quasi-particle states, for which $\int d\mathbf{r} |v_k(\mathbf{r}, \sigma)|^2 < \infty$ in the final nucleus or in the fission fragment. If the sum in the definition of $\hat{\mathcal{Q}}$ would have been restricted to $E_k > 0$, only the occupied quasi-particle states in the ground state of the nucleus or fragment would have been included. In the case of a HFB framework the quasiparticle spectrum is continuous for both occupied and unoccupied quasi-particle states if $|E_k| > |\mu|$ and the projector $\hat{\mathcal{P}}$ selects only the unbound unoccupied quasi-particle states with $E_k < \mu$, when $\int d\mathbf{r} |v_k(\mathbf{r}, \sigma)|^2 \rightarrow \infty$.

The Eqs. (8) and (9) read in this case [22]

$$P(n) = \int_{-\pi}^{\pi} \frac{d\eta}{2\pi} e^{-i\eta n} \sqrt{\det[\delta_{kl} + (e^{i\eta} - 1)P_{kl}]}, \quad (46)$$

$$Q(n') = \int_{-\pi}^{\pi} \frac{d\eta}{2\pi} e^{-i\eta n'} \sqrt{\det[\delta_{kl} + (e^{i\eta} - 1)Q_{kl}]}, \quad (47)$$

where

$$P_{kl} = \langle\phi_k|\hat{\mathcal{P}}|\phi_l\rangle, \quad Q_{kl} = \langle\phi_k|\hat{\mathcal{Q}}|\phi_l\rangle \quad (48)$$

and $\phi_k(x)$ are now the 4-components Bogoliubov quasi-particle wave functions obtained by evolving Eqs. (42). After orthogonalizing $\langle\phi_k|\hat{\mathcal{P}}|\phi_l\rangle$ and $\langle\phi_k|\hat{\mathcal{Q}}|\phi_l\rangle$ these expressions simplify

$$P(n) = \int_{-\pi}^{\pi} \frac{d\eta}{2\pi} e^{-i\eta n} \sqrt{\prod_{k=1}^{2\Omega} [1 + (e^{i\eta} - 1)\alpha_k^2]}, \quad (49)$$

$$Q(n') = \int_{-\pi}^{\pi} \frac{d\eta}{2\pi} e^{-i\eta n'} \sqrt{\prod_{l=1}^{2\Omega} [1 + (e^{i\eta} - 1)\beta_l^2]}, \quad (50)$$

where

$$\alpha_k^2 = \langle\phi_k|\hat{\mathcal{P}}|\phi_k\rangle, \quad \beta_k^2 = \langle\phi_k|\hat{\mathcal{Q}}|\phi_k\rangle, \quad (51)$$

and 2Ω is the dimension of the Fock space. The total number of pre-equilibrium neutrons evaporated can be determined either from $\nu = \sum_{n=0}^{\infty} nP(n)$ or as

$$\nu = \sum_k \langle\phi_k|\hat{\mathcal{P}}|\phi_k\rangle. \quad (52)$$

If instead one uses a TDHF-BCS framework [38, 48–50] to describe the initial nucleus then

$$v_k(x, t) = v_k(t)\phi_k(x, t), \quad u_k(x, t) = u_k(t)\phi_k(x, t) \quad (53)$$

$|v_k(t)|^2$ are the occupation probabilities, $\phi_k(x, t)$ are 2-components single-particle wave functions obtained as solutions of the TDHF equations, $\langle\phi_k|\phi_l\rangle = \delta_{kl}$, and $|v_k(t)|^2 + |u_k(t)|^2 = 1$.

III. CONCLUSIONS

The formalism outlined here can be used to characterize the fate of the quasi-particle states promoted into the continuum either in an excited nucleus or in an excited nuclear fragment. One can calculate for each quasiparticle state, initially localized inside the nucleus, an averaged transmission probability into the continuum. These transmission probabilities lead to upper estimates of the number of the pre-equilibrium neutrons emitted, up to corrections due to the branching ratio Γ^\dagger/Γ . The only other source of uncertainties is due to the role of fluctuations, which is expected to lead to wider distributions, but it will likely not affect radically the average neutron

multiplicities [35–38]. The role of fluctuations can be accounted for in a variety of ways [36, 51–58]. The extension to emission of other kind of particles is straightforward.

The formalism can be extended to project other single-particle properties, such as the energies of the emitted nucleons, and/or their angular momenta in a manner discussed in Refs. [22, 24, 59]². By projecting the linear momenta of the emitted nucleons one can obtain simultaneously the angular and the energy distributions of

the emitted nucleons.

ACKNOWLEDGEMENTS

I thank G.F. Bertsch for discussions and N. Carjan and I. Stetcu for urging me to think about this problem. This work was supported by U.S. Department of Energy, Office of Science, Grant No. DE-FG02-97ER41014 and in part by NNSA cooperative Agreement DE-NA0003841.

-
- [1] L. Meitner, “Über die Entstehung der β -Strahl-Spektren radioactiver Substanzen,” *Z. Phys.* **9**, 131 (1922).
- [2] P. Auger, “Sur les rayons β^- secondaires produits dans un gaz par des rayons X,” *C.R.A.S.* **177**, 166 (1923).
- [3] L. D. Landau and E. M. Lifshitz, *Quantum Mechanics: Non-relativistic theory*, 3rd ed., Course of Theoretical Physics, Vol. 3 (Butterworth-Heinemann, Oxford, 2003, c1977).
- [4] N. Carjan and M. Rizea, “Scission neutrons and other scission properties as function of mass asymmetry in $^{235}\text{U}(n_{\text{th}}, f)$,” *Phys. Rev. C* **82**, 014617 (2010).
- [5] N. Carjan, F.-J. Hamsch, M. Rizea, and O. Serot, “Partition between the fission fragments of the excitation energy and of the neutron multiplicity at scission in low-energy fission,” *Phys. Rev. C* **85**, 044601 (2012).
- [6] M. Rizea and N. Carjan, “Dynamical scission model,” *Nucl. Phys. A* **909**, 50 (2013).
- [7] N. Carjan and M. Rizea, “Similarities between calculated scission-neutron properties and experimental data on prompt fission neutrons,” *Phys. Lett. B* **747**, 178 (2015).
- [8] R. Capote, N. Carjan, and S. Chiba, “Scission neutrons for U, Pu, Cm, and Cf isotopes: Relative multiplicities calculated in the sudden limit,” *Phys. Rev. C* **93**, 024609 (2016).
- [9] N. Carjan and M. Rizea, “Structures in the energy distribution of the scission neutrons: Finite neutron-number effect,” *Phys. Rev. C* **99**, 034613 (2019).
- [10] N. Carjan and M. Rizea, “Acceleration induced neutron emission in heavy nuclei (unpublished, presented at *26th International Seminar on Interaction of Neutrons with Nuclei*, Xi’an, PR China, May 28-June 1, 2018).”
- [11] M.G. Mustafa, H.W. Schmitt, and U. Mosel, “Dipole excitations in fission fragments,” *Nucl. Phys. A* **178**, 9 (1971).
- [12] C. Simenel and A. S. Umar, “Formation and dynamics of fission fragments,” *Phys. Rev. C* **89**, 031601 (2014).
- [13] H. F. Hess, “Evaporative cooling of magnetically trapped and compressed spin-polarized hydrogen,” *Phys. Rev. B* **34**, 3476 (1986).
- [14] R. van Roijen, J. J. Berkhout, S. Jaakkola, and J. T. M. Walraven, “Experiments with atomic hydrogen in a magnetic trapping field,” *Phys. Rev. Lett.* **61**, 931 (1988).
- [15] N. Masuhara, J. M. Doyle, J. C. Sandberg, D. Kleppner, T. J. Greytak, H. F. Hess, and G. P. Kochanski, “Evaporative cooling of spin-polarized atomic hydrogen,” *Phys. Rev. Lett.* **61**, 935 (1988).
- [16] J. M. Doyle, J. C. Sandberg, I. A. Yu, C. L. Cesar, D. Kleppner, and T. J. Greytak, “Hydrogen in the submillikelvin regime: Sticking probability on superfluid ^4He ,” *Phys. Rev. Lett.* **67**, 603 (1991).
- [17] I. D. Setija, H. G. C. Werij, O. J. Luiten, M. W. Reynolds, T. W. Hijmans, and J. T. M. Walraven, “Optical cooling of atomic hydrogen in a magnetic trap,” *Phys. Rev. Lett.* **70**, 2257 (1993).
- [18] K. B. Davis, M.-O. Mewes, M. A. Joffe, M. R. Andrews, and W. Ketterle, “Evaporative cooling of sodium atoms,” *Phys. Rev. Lett.* **74**, 5202 (1995).
- [19] W. Petrich, M. H. Anderson, J. R. Ensher, and E. A. Cornell, “Stable, tightly confining magnetic trap for evaporative cooling of neutral atoms,” *Phys. Rev. Lett.* **74**, 3352 (1995).
- [20] E. A. Cornell and C. E. Wieman, “Nobel lecture: Bose-einstein condensation in a dilute gas, the first 70 years and some recent experiments,” *Rev. Mod. Phys.* **74**, 875 (2002).
- [21] W. Ketterle, “Nobel lecture: When atoms behave as waves: Bose-einstein condensation and the atom laser,” *Rev. Mod. Phys.* **74**, 1131 (2002).
- [22] A. Bulgac, “Projection of Good Quantum Numbers for Reaction Fragments,” *Phys. Rev. C* **100**, 034612 (2019).
- [23] C. Simenel, “Particle Transfer Reactions with the Time-Dependent Hartree-Fock Theory Using a Particle Number Projection Technique,” *Phys. Rev. Lett.* **105**, 192701 (2010).
- [24] K. Sekizawa and K. Yabana, “Particle-number projection method in time-dependent Hartree-Fock theory: Properties of reaction products,” *Phys. Rev. C* **90**, 064614 (2014).
- [25] J. Blocki, Y. Boneh, J. R. Nix, J. Randrup, M. Robel, A. J. Sierk, and W. J. Swiatecki, “One-body dissipation and the super-viscosity of nuclei,” *Ann. Phys.* **113**, 330 (1978).
- [26] A. Bulgac, S. Jin, K. J. Roche, N. Schunck, and I. Stetcu, “Fission dynamics of ^{240}Pu from saddle to scission and beyond,” *Phys. Rev. C* **100**, 034615 (2019).

² In Ref. [59] the bound and unbound nucleons are discriminated by their spatial distribution, not by their single-particle energies, as suggested here, and that can lead in principle to different results.

- [27] A. Bulgac, S. Jin, and I. Stetcu, “Nuclear Fission Dynamics: Past, Present, Needs, and Future,” *Frontiers in Physics* **8**, 63 (2020).
- [28] W. Belzig, C. Schroll, and C. Bruder, “Density correlations in ultracold atomic fermi gases,” *Phys. Rev. A* **75**, 063611 (2007).
- [29] D. Lacroix and S. Ayik, “Counting statistics in finite Fermi systems: Illustrations with the atomic nucleus,” *Phys. Rev. C* **101**, 014310 (2020).
- [30] F. M. Marqués, M. Labiche, N. A. Orr, J. C. Angélique, L. Axelsson, B. Benoit, U. C. Bergmann, M. J. G. Borge, W. N. Catford, S. P. G. Chappell, N. M. Clarke, G. Costa, N. Curtis, A. D’Arrigo, E. de Góes Brennand, F. de Oliveira Santos, O. Dorvaux, G. Fazio, M. Freer, B. R. Fulton, G. Giardina, S. Grévy, D. Guillemaud-Mueller, F. Hanappe, B. Heusch, B. Jonson, C. Le Brun, S. Leenhardt, M. Lewitowicz, M. J. López, K. Markenroth, A. C. Mueller, T. Nilsson, A. Ninane, G. Nyman, I. Piqueras, K. Riisager, M. G. Saint Laurent, F. Sarazin, S. M. Singer, O. Sorlin, and L. Stuttgé, “Detection of neutron clusters,” *Phys. Rev. C* **65**, 044006 (2002).
- [31] H.J. Rose and G.A. Jones, “A new kind of natural radioactivity,” *Nature* **307**, 245 (1984).
- [32] A. Sandulescu, D.N. Poenaru, and W. Greiner, “New type of decay of heavy nuclei intermediate between fission and alpha-decay,” *Sov. J. Part. Nucl.* **11**, 528 (1980).
- [33] R. Y. Cusson, P. G. Reinhard, M. R. Strayer, J. A. Maruhn, and W. Greiner, “Density as a constraint and the separation of internal excitation energy in TDHF,” *Z. Phys. A* **320**, 475 (1985).
- [34] G. F. Bertsch, P. F. Bortignon, and R. A. Broglia, “Damping of nuclear excitations,” *Rev. Mod. Phys.* **55**, 287 (1983).
- [35] R. Balian and M. Vénéroni, “Fluctuations in a time-dependent mean-field approach,” *Phys. Lett. B* **136**, 301 (1984).
- [36] A. Bulgac, S. Jin, and I. Stetcu, “Unitary evolution with fluctuations and dissipation,” *Phys. Rev. C* **100**, 014615 (2019).
- [37] C. Simenel, “Particle-Number Fluctuations and Correlations in Transfer Reactions Obtained Using the Balian-Vénéroni Variational Principle,” *Phys. Rev. Lett.* **106**, 112502 (2011).
- [38] C. Simenel and A.S. Umar, “Heavy-ion collisions and fission dynamics with the time-dependent Hartree-Fock theory and its extensions,” *Progress in Particle and Nuclear Physics* **103**, 19 (2018).
- [39] V.M. Strutinsky, “Shell effects in nuclear masses and deformation energies,” *Nucl. Phys. A* **95**, 420 (1967).
- [40] M. Brack, J. Damgaard, A. S. Jensen, H. C. Pauli, V. M. Strutinsky, and C. Y. Wong, “Funny Hills: The Shell-Correction Approach to Nuclear Shell Effects and Its Applications to the Fission Process,” *Rev. Mod. Phys.* **44**, 320 (1972).
- [41] S. Jin, A. Bulgac, K. Roche, and G. Wlazłowski, “Coordinate-space solver for superfluid many-fermion systems with the shifted conjugate-orthogonal conjugate-gradient method,” *Phys. Rev. C* **95**, 044302 (2017).
- [42] A. Bulgac, “Hartree-Fock-Bogoliubov approximation for finite systems (1980),” [arXiv:nucl-th/9907088](https://arxiv.org/abs/nucl-th/9907088).
- [43] J. Dobaczewski, H. Flocard, and J. Treiner, “Hartree-Fock-Bogolyubov description of nuclei near the neutron drip line,” *Nucl. Phys. A* **422**, 103 (1984).
- [44] S.T. Belyaev, A.V. Smirnov, S.V. Tolokonnikov, and S.A. Fayans, “Pairing in nuclei in the coordinate representation,” *Sov. J. Nucl. Phys.* **45**, 783 (1987).
- [45] J. Dobaczewski, W. Nazarewicz, T. R. Werner, J. F. Berger, C. R. Chinn, and J. Dechargé, “Mean-field description of ground-state properties of drip-line nuclei: Pairing and continuum effects,” *Phys. Rev. C* **53**, 2809–2840 (1996).
- [46] I. Stetcu, C. Bertulani, A. Bulgac, P. Magierski, and K. J. Roche, “Relativistic Coulomb excitation within Time Dependent Superfluid Local Density Approximation,” *Phys. Rev. Lett.* **114**, 012701 (2015).
- [47] T. Nakatsukasa, K. Matsuyanagi, M. Matsuo, and K. Yabana, “Time-dependent density-functional description of nuclear dynamics,” *Rev. Mod. Phys.* **88**, 045004 (2016).
- [48] G. Scamps, D. Lacroix, G.F. Bertsch, and K. Washiyama, “Pairing dynamics in particle transport,” *Phys. Rev. C* **85**, 034328 (2012).
- [49] G. Scamps and D. Lacroix, “Effect of pairing on one- and two-nucleon transfer below the Coulomb barrier: A time-dependent microscopic description,” *Phys. Rev. C* **87**, 014605 (2013).
- [50] K. Sekizawa, “TDHF Theory and Its Extensions for the Multinucleon Transfer Reaction: A Mini Review,” *Frontiers in Physics* **7**, 20 (2019).
- [51] P. Grangé, J.-Q. Li, and H. A. Weidenmüller, “Induced nuclear fission viewed as a diffusion process: Transients,” *Phys. Rev. C* **27**, 2063 (1983).
- [52] H. A. Weidenmüller and J.-S. Zhang, “Nuclear fission viewed as a diffusion process: Case of very large friction,” *Phys. Rev. C* **29**, 879 (1984).
- [53] P. Fröbrich and I.I. Gontchar, “Langevin description of fusion, deep-inelastic collisions and heavy-ion-induced fission,” *Phys. Rep.* **292**, 131 (1998).
- [54] J. Randrup and P. Möller, “Brownian Shape Motion on Five-Dimensional Potential-Energy Surfaces:Nuclear Fission-Fragment Mass Distributions,” *Phys. Rev. Lett.* **106**, 132503 (2011).
- [55] D. E. Ward, B. G. Carlsson, T. Døssing, P. Möller, J. Randrup, and S. Åberg, “Nuclear shape evolution based on microscopic level densities,” *Phys. Rev. C* **95**, 024618 (2017).
- [56] A. J. Sierk, “Langevin model of low-energy fission,” *Phys. Rev. C* **96**, 034603 (2017).
- [57] C. Ishizuka, M. D. Usang, F. A. Ivanyuk, J. A. Maruhn, K. Nishio, and S. Chiba, “Four-dimensional Langevin approach to low-energy nuclear fission of ^{236}U ,” *Phys. Rev. C* **96**, 064616 (2017).
- [58] M. Albertsson, B.G. Carlsson, T. Døssing, P. Möller, J. Randrup, and S. Åberg, “Excitation energy partition in fission,” *Phys. Lett. B* **803**, 135276 (2020).
- [59] B. Avez and C. Simenel, “Structure and direct decay of Giant Monopole Resonances,” *Eur. Phys. J. A* **49**, 76 (2013).